08,05,13

The Influence of Ti Doping at the Mn Site on Magnetoresistance and Thermopower Properties of $Nd_{0.5}Ca_{0.5}MnO_3$

© A. Anand, M. Manjuladevi, R.K. Veena, V.S. Veena, S. Sagar¶

Department of Physics, Govt College for Women, Vazhuthacaud, Research Centre, University of Kerala, Thiruvananthapuram, Kerala, India

¶ E-mail: sagargcw@gmail.com

Received: January 14, 2022
Revised: January 14, 2022
Accepted: January 22, 2022

Nd-Ca-based manganite $Nd_{0.5}Ca_{0.5}MnO_3$ and 10% Ti-doped manganite $Nd_{0.5}Ca_{0.5}Ti_{0.1}Mn_{0.9}O_3$ denoted by N and $N_{0.1}$, respectively, were prepared using solid-state reaction method. Resistivity gets increased for the Ti-doped sample. The parent compound N has remarkably high magnetoresistance. The highest value of Seebeck coefficient for N is $-97\,\mu VK^{-1}$ at 143 K and for $N_{0.1}$ is $-207\,\mu VK^{-1}$ at 203 K. Variable range hopping mechanism successfully explains the high temperature resistivity and thermopower data.

Keywords: magnetoresistance, thermoelectric power, rare-earth based manganites, manganites.

DOI: 10.21883/PSS.2022.06.54371.001

1. Introduction

Active exploration of energy sources other than fossil fuels is the necessity of the current world. Thermoelectric power (TEP) technology opens a way to convert a temperature change directly into electric voltage. It has been an emerging technology during the last two decades and attracted considerable attention due to its possibility of converting waste heat into electrical power and enhancing fuel efficiency. The Seebeck effect discovered by Thomas Johann Seebeck in 1821 is the principle behind thermoelectric power generation [1]. When a conductor is subjected to a temperature gradient, an electric voltage will generate. The generated voltage is called thermoelectric voltage, and its rate of change with respect to the temperature is a constant known as the Seebeck coefficient S.

$$S = -(dV/dT). \tag{1}$$

When a temperature gradient is applied across a conductor, charge carriers will flow from the hot end to the cold end. The accumulation of more charges at the cold end than the hot end will create an inhomogeneous charge distribution, and it creates an electric field that opposes the further diffusion of charge carriers from the hot end to the cold end. If the material is in an open circuit, the diffusion of charge carriers from hot end to the cold end will be balanced by the movement of charge carriers in the reverse direction due to the effect of the electric field and an equilibrium is achieved. In this equilibrium condition, the thermoelectric potential difference formed due to the temperature gradient is known as Seebeck voltage. The amount of voltage generated per unit temperature gradient is called the Seebeck coefficient [2]. When this thermoelectric material under the application of a temperature gradient is connected to a circuit, the generated Seebeck voltage can drive a current through the circuit and can be used to perform electrical work [3, 4]. The efficiency of a thermoelectric material is determined by the figure of merit (ZT) term which is a function of its transport coefficients and it is defined as follows:

$$ZT = \frac{S^2\sigma}{\kappa}T, \tag{2}$$

where S is the Seebeck coefficient, σ is the electrical conductivity, T is the absolute temperature and κ is the corresponding thermal conductivity. Since TEP has application in waste heat recovery in the industrial and automobile sector, development in this field has a potential impact on the earth.

Magnetoresistance (MR) of a material is the change in resistance in response to the application of an external magnetic field. Mixed valent manganites are well known for their remarkable magnetoresistance property. The concentrations of both Mn^{3+} and Mn^{4+} ions determine the double exchange mechanism in rare-earth manganites, which plays a vital role in the magnetoresistance property of the corresponding material.

Rare-earth-based mixed valent perovskite manganites are well known for their thermopower and magnetoresistance properties. Half-doped Nd–Ca-based manganite $Nd_{0.5}Ca_{0.5}MnO_3$ is an interesting compound due to its exciting electric and magnetic properties [5–7] and is seldom studied for its thermopower properties. The equal concentration of Mn^{3+} and Mn^{4+} may give exciting MR properties for this compound. The rare-earth-based titanate compound $SrTiO_3$ is extensively studied for its TEP properties, in which Ti ions have a crucial role in the conduction mechanism. Hence doping of Ti ions at the Mn site of $Nd_{0.5}Ca_{0.5}MnO_3$ will alter its thermopower properties. Here we report the influence of Ti doping at the Mn site on magnetoresistance and thermopower properties of $Nd_{0.5}Ca_{0.5}MnO_3$.

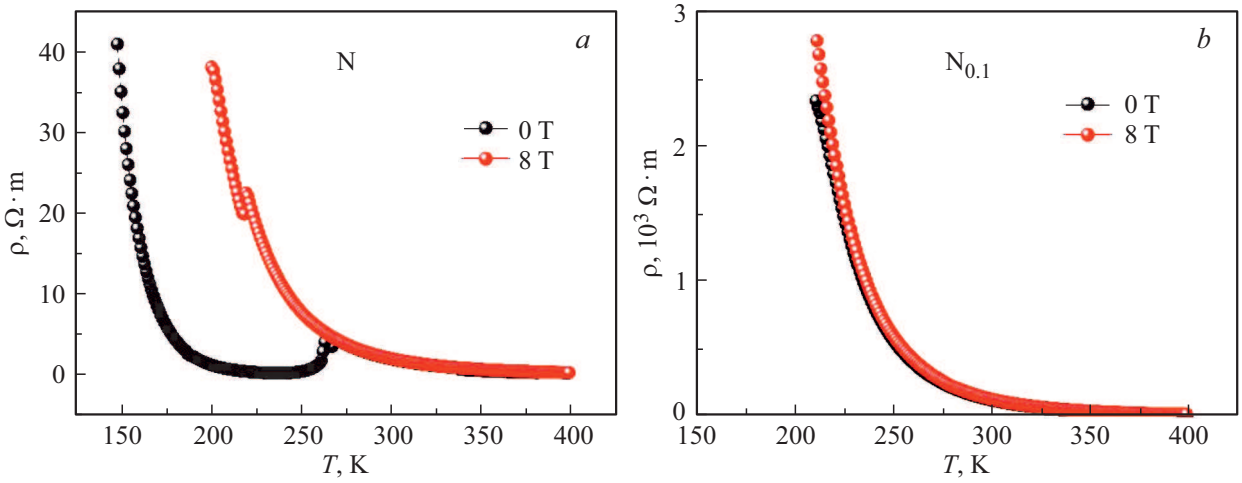

Figure 1. Temperature-dependent resistivity variations under 0 and 8 T for samples N and $N_{0.1}$, respectively.

2. Experimental details

The Nd-Ca-based manganite $Nd_{0.5}Ca_{0.5}MnO_3$ and the 10% Ti-doped compound $Nd_{0.5}Ca_{0.5}Ti_{0.1}Mn_{0.9}O_3$ denoted by N and $N_{0.1}$ were prepared by conventional solid state reaction method. The high-purity precursors such as the oxides and carbonates of the constituent elements were thoroughly mixed under acetone medium for 9 hours; calcination of powder samples and sintering of pressed pellets were carried out at 900 and 1200°C, respectively, for 24 hours. The detailed discussion on the preparation method and the structural analysis were already reported [5, 8]. Resistance as a function of temperature was measured using Quantum design PPMS instrument, from which the corresponding resistivity is calculated from the dimensions of the sample. Variation of Seebeck coefficients with temperature was measured by using a customized measurement setup which is fabricated to be compatible with low cooling power systems such as 4 K Close Cycle Refrigerators (CCRs) [9].

3. Results and discussions

3.1. Resistivity and magnetoresistance analysis

DC resistivities of the samples as a function of temperatures were calculated from temperature-dependent DC-resistance data measured by the four-probe method using the dimensions of the samples. To analyze MR properties, resistance variations with temperature under an applied magnetic field of 8 T are also measured. Temperature-dependent DC-resistivities of samples N and under 0 and 8 T are given in Fig. 1, *a* and *b*. From Fig. 4, it is clear that the resistivity values drastically increase with Ti-doping due to the increase in the concentration of non-magnetic Ti-ions. Due to the limitation of the measurement system, resistivity data of the samples were measured only up to the possible low-temperature values. To compare the resistivity and MR data, resistivities of all three samples are presented in a common temperature range. Parent compound N shows a significant zero-field resistivity variation at 270 K which is above the charge-ordering temperature ($T_{CO} = 235$ K) of the compound [5]. As the temperature decreases, resistivity starts to rise around its Neel temperature ($T_N = 140$ K), which may be due to the AFM orderings in the sample. Under the magnetic field of 8 T, a slight drop in resistivity occurs at comparatively lower temperature (219 K). A significant variation between the resistivity data at 0 and 8 T points to a remarkable MR. The Ti-doped sample $N_{0.1}$ has gradually increased resistivities below 300 K, and even under the application of an external magnetic field (8 T) there is no significant difference between the values of resistivities.

DC resistivity data of the samples can be analyzed using both small polaron hopping (SPH) and variable range hopping (VRH) mechanisms. SPH mechanism suggests multi phonon-assisted hopping for electric conduction [10]. According to the SPH mechanism, variation of resistivity with temperature can fit using the following equation:

$$\rho = AT \exp\left(\frac{E_A}{k_B T}\right), \tag{3}$$

where E_A is the activation energy for hopping and A is a constant. Resistivity data plotted by taking $\ln(\rho/T)$ and

Table 1. Fitting parameters obtained from SPH theoretical fit according to equation (3).

Samples	Magnetic field, T	R^2	E_A, meV	A, ΩmK^{-1}
N	0	0.99823	193	$8.8464 \cdot 10^{-8}$
	8	0.99606	192	$3.8507 \cdot 10^{-6}$
$N_{0.1}$	0	0.99748	230	$4.9574 \cdot 10^{-3}$
	8	0.99778	232	$4.9371 \cdot 10^{-3}$

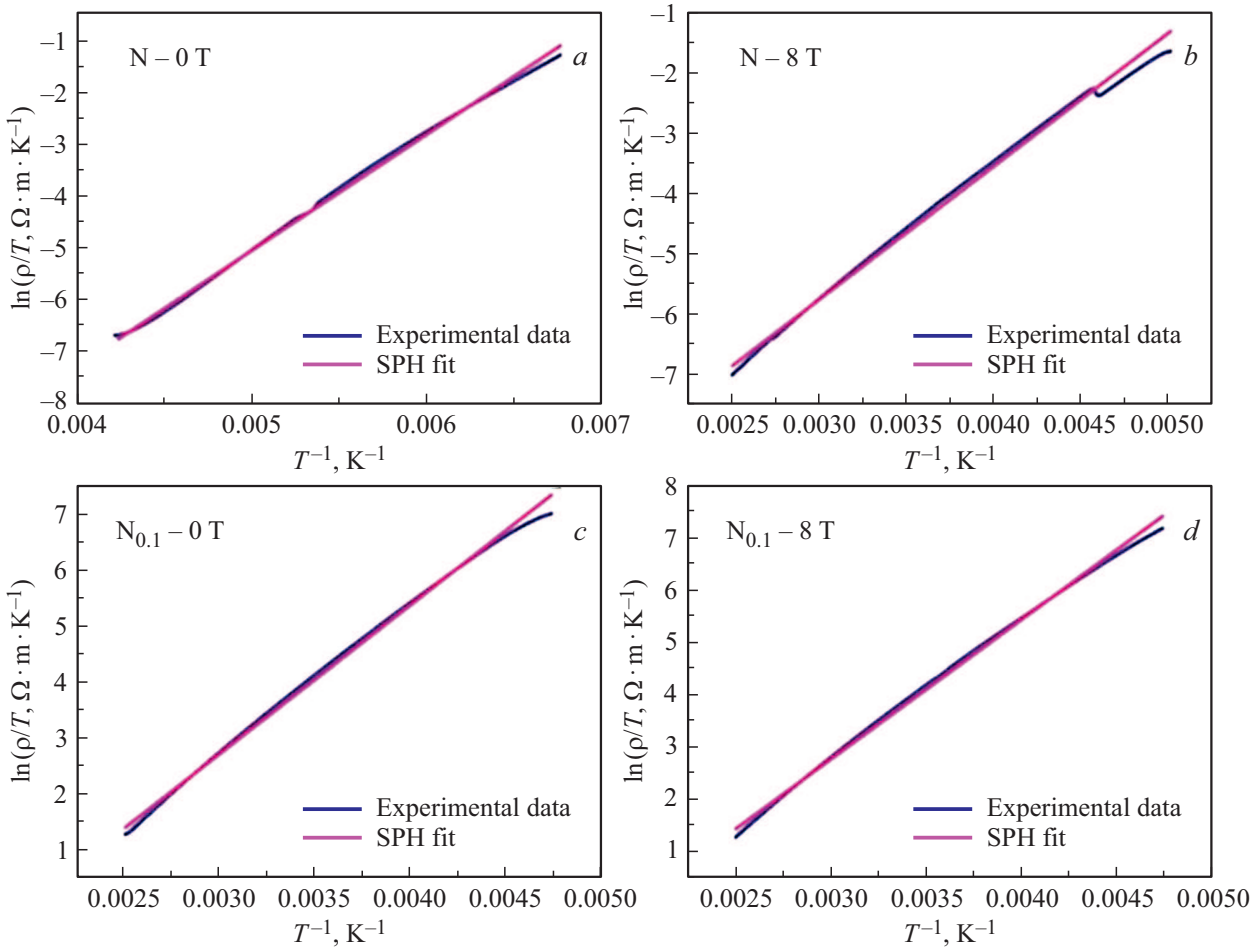

Figure 2. High-temperature experimental resistivity data along with the theoretical fit according to SPH model for samples N and $N_{0.1}$ at 0 and 8 T.

$(1/T)$ along the two axes with the corresponding theoretical fit based on equation (3) are depicted in Fig. 2, $a-d$. The resultant fitting parameters are tabulated in Table 1. From Table 1, it is clear that the value of activation energy increases with Ti doping.

According to the VRH model, the electrons can hop from one site to another with the help of phonons if the electrons are not deeply trapped. The temperature-dependent resistivity variation according to this model is given by equation (4).

$$\rho = \rho_0 \exp\left(\frac{T_0}{T}\right)^{1/4}. \quad (4)$$

The experimental data and the theoretical fit according to equation (4) for 0 and 8 T for the samples N and $N_{0.1}$ are depicted in Fig. 3, $a-d$, and the fitting parameters obtained are tabulated in Table 2. From Fig. 3, $a-d$, it is clear that the VRH fit is in better agreement with the experimental data than the SPH fit. By considering the goodness of fit (R^2), the VRH model can be successfully used to analyze the high-temperature resistivity data of the three samples.

Table 2. Fitting parameters obtained from VRH theoretical fit according to equation (4).

Samples	Magnetic field, T	R^2	ρ_0, Ωm	T_0, K
N	0	0.98479	$0.7381 \cdot 10^{-12}$	119.0970
	8	0.99870	$2.5187 \cdot 10^{-12}$	114.3976
$N_{0.1}$	0	0.99956	$76.8660 \cdot 10^{-12}$	136.0603
	8	0.99961	$64.2493 \cdot 10^{-12}$	137.0869

Magnetoresistance (for an applied magnetic field of 8 T) as a function of temperature for the samples were calculated from the temperature-dependent resistivity data at magnetic fields 0 and 8 T using equation (5):

$$MR(\%) = \frac{R(H) - R(0)}{R_0} \cdot 100, \quad (5)$$

where $R(H)$ and $R(0)$ are the resistances of the sample with and without magnetic field. The corresponding variations

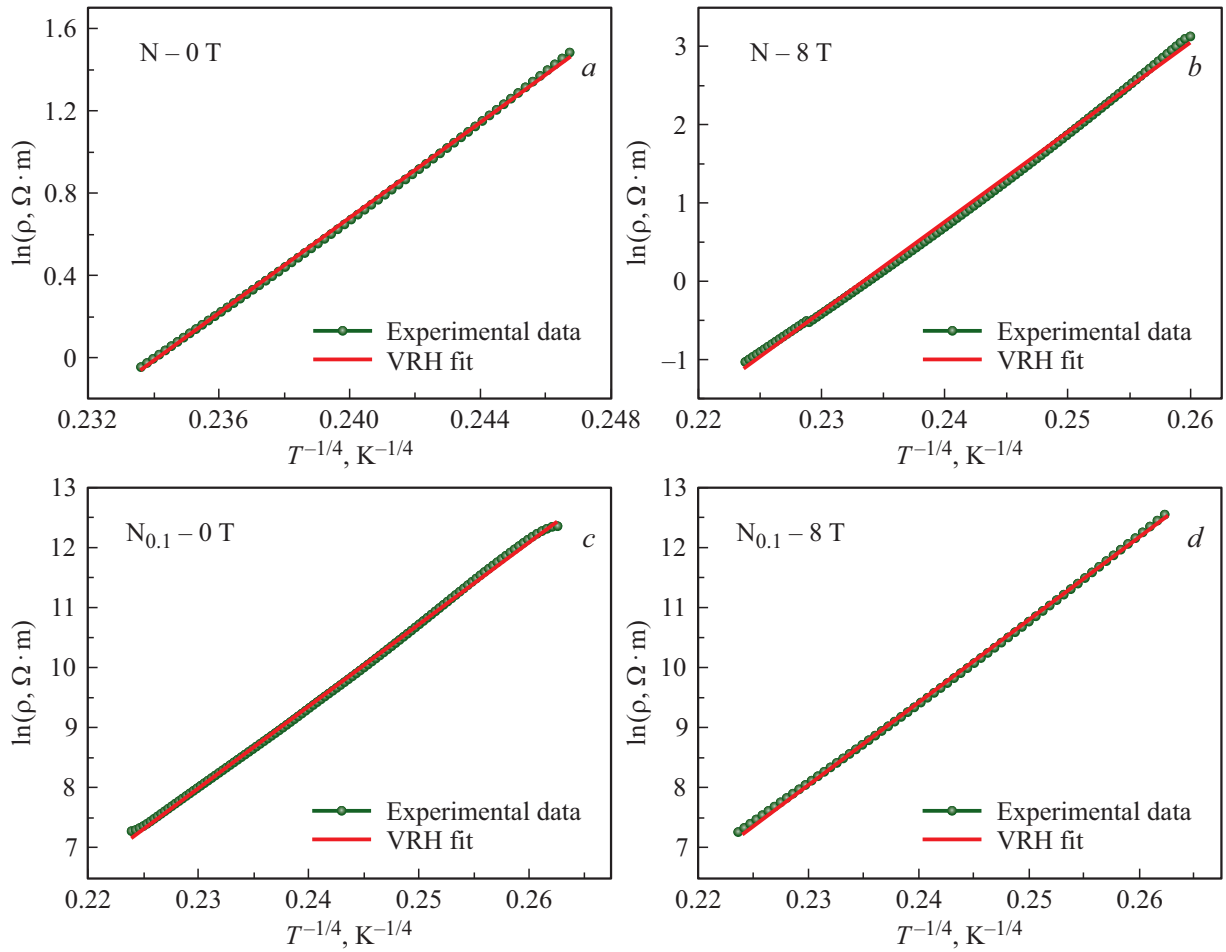

Figure 3. High-temperature experimental resistivity data along with the theoretical fit according to VRH model for samples N and $N_{0.1}$ at 0 and 8 T.

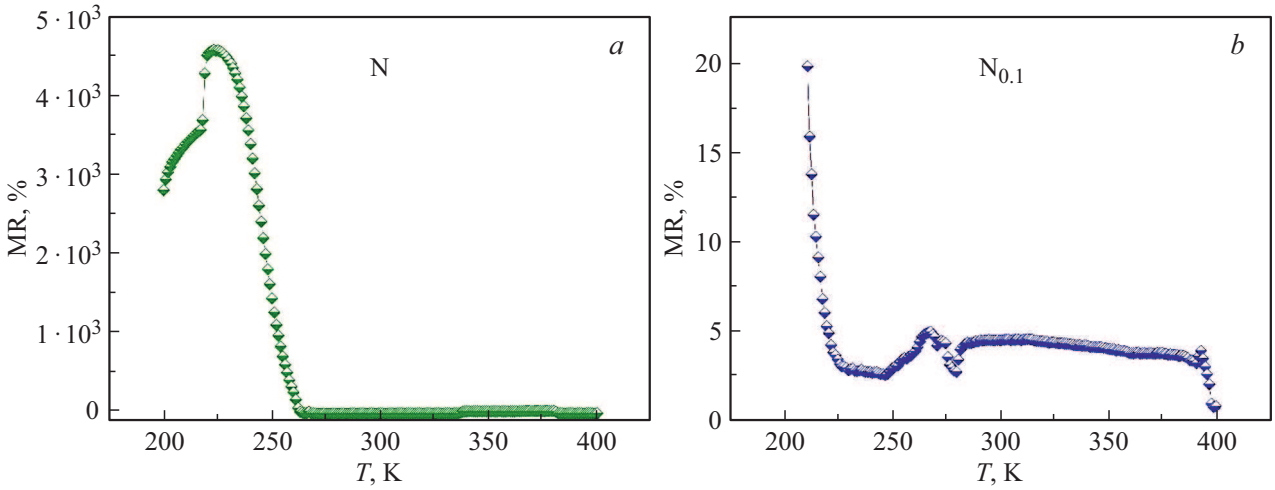

Figure 4. Variation of temperature-dependent magnetoresistances (MR%) at 8 T for samples N and $N_{0.1}$, respectively.

for the samples are shown in Fig. 4, *a* and *b*. The parent compound N exhibits a very high magnetoresistance at 223 K. Such huge magnetoresistance was already reported in similar manganite $Sm_{0.5}Ca_{0.25}Sr_{0.25}MnO_3$ [11]. For the Ti-doped sample $N_{0.1}$, MR values drop significantly. Another small dip of MR originated around 275 K for the Ti-doped manganites $N_{0.1}$. Since there is no significant magnetisation variation for $N_{0.1}$ at 275 K in the corresponding M–T

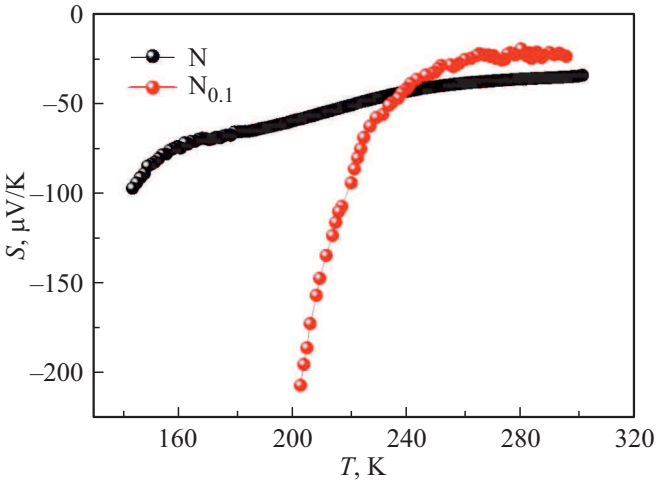

Figure 5. Variation of Seebeck coefficient with temperature for samples N and $N_{0.1}$.

curve [8], these MR peaks do not have a magnetic origin.

3.2. Thermopower analysis

To investigate the effect of Ti doping on the thermoelectric power (TEP) properties of the current samples, Seebeck coefficients S as a function of temperature were measured. High resistivity of the samples at low temperatures limited the measurement of S at low temperatures of the samples N and $N_{0.1}$. The variations of S with temperature for samples N and $N_{0.1}$ are depicted in Fig. 5. Sample N attains a high value of $S = -97\mu\,\mathrm{VK}^{-1}$ at 143 K, and sample $N_{0.1}$ attains $S = -207\,\mu\mathrm{VK}^{-1}$ at 203 K. Thus, the presence of Ti increases the temperature corresponding to the high value of S. The negative values of S indicate that electrons are the charge carriers responsible for conduction in the corresponding temperature region.

Table 3. Fitting parameters obtained from theoretical fit on TEP data based on VRH model for samples N and $N_{0.1}$.

Samples	R^2	S_0, $\mu\mathrm{VK}^{-1}$	K, $\mu\mathrm{VK}^{-3/2}$
N	0.99825	−228.4546	11.8975
$N_{0.1}$	0.94315	−542.0826	32.1443

Since the VRH model gives a better theoretical fit for the high-temperature resistivity data than the SPH mechanism, high-temperature TEP data is also analysed using the VRH mechanism. The following equation can define the variation of the high-temperature Seebeck coefficient according to the VRH model [12, 13].

$$S = S_0 + K(T)^{1/2}, \tag{6}$$

where $K = \frac{k_B}{3e}\xi^2 T_0^{1/2}[d\ln N(\varepsilon)/d\varepsilon]$, ε is the energy measured at the Fermi level, ξ is the factor that determines the width of the energy layer within which the states are effective in conduction, and T_0 is the characteristic temperature.

Experimental TEP data along with the VRH fit at higher temperature regions of samples N and $N_{0.1}$ are depicted in Fig. 6, *a* and *b*, respectively. The corresponding fitting parameters obtained were also tabulated in Table 3. Thus, similar to the resistivity data, high-temperature TEP data can also be explained using the VRH mechanism.

4. Conclusion

Half-doped Nd-Ca based manganite $Nd_{0.5}Ca_{0.5}MnO_3$ and 10% Ti-doped sample $Nd_{0.5}Ca_{0.5}Ti_{0.1}Mn_{0.9}O_3$ were prepared using conventional solid-state reaction method. Resistivities of the samples as a function of temperature were measured. Ti doping increases the resistivities of

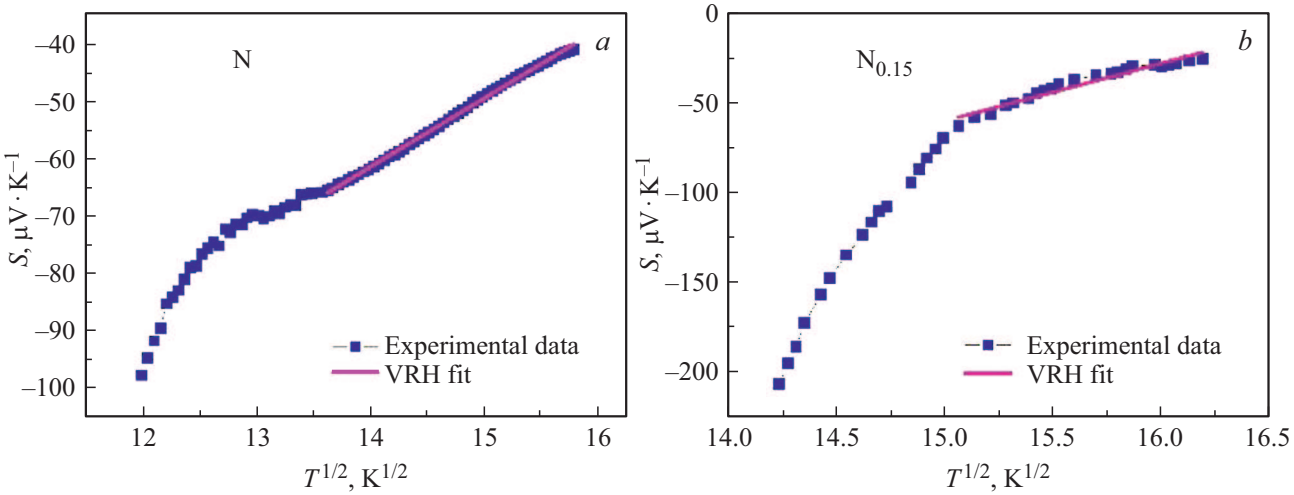

Figure 6. Experimental TEP data along with the theoretical fit based on VRH model for samples N and $N_{0.1}$, respectively.

the samples. The parent sample N has remarkably high magnetoresistance and the MR values drastically drop for the Ti-doped sample $N_{0.1}$. The Seebeck coefficient (S) of sample N attains a high value of $-97\,\mu VK^{-1}$ at 143 K, and the same for sample $N_{0.1}$ attains a high value of $S = -207\,\mu VK^{-1}$ at 203 K. High-temperature resistivity data and TEP data can be successfully explained by using the VRH model.

Author contribution

A. Anand: conceptualization, methodology, and original draft preparation; A. Anand, M. Manjuladevi, R.K. Veena, and V.S. Veena: formal analysis and investigation; A. Anand and S. Sagar: review and editing; S. Sagar: supervision.

Acknowledgment

We acknowledge Dr. V. Ganesan and Dr. R. Venkatesh, UGC-DAE-CSR Indore for thermoelectric power and resistivity measurements. One of the authors (Anitha Anand) acknowledges University of Kerala for Junior Research Fellowship.

Conflict of interest

The authors declare that they have no conflicts of interest.

References

[1] T.J. Seebeck. Abhand. Deut. Akad. Wiss., 265 (1822).
[2] A.J. Minnich, M.S. Dresselhaus, Z.F. Ren, and G. Chen. Energy Environ. Sci. **2**, *5*, 466 (2009). http://dx.doi.org/10.1039/b822664b
[3] G.S. Nolas, J. Shar, and H. Goldsmid. Thermoelectrics: Basic Principles and New Materials Developments. Springer, N.Y. (2001).
[4] D. Rowe (Ed.). Thermoelectrics Handbook: Macro to Nano. CRC Press, Boca Raton (2006).
[5] A. Anand, M. Manjuladevi, R.K. Veena, V.S. Veena, Y.S. Koshkid'ko, and S.J. Sagar. J. Magn. Magn. Mater. **528**, 167810 (2021). https://doi.org/10.1016/j.jmmm.2021.167810
[6] F. Millange, S. de Brion, and G. Chouteau. Phys. Rev. B **62**, *9*, 5619 (2000). https://doi.org/10.1103/PhysRevB.62.5619
[7] H. Trabelsi. J. Rare Earths **38**, *10*, 1076 (2020). https://doi.org/10.1016/j.jre.2019.10.004
[8] A. Anand, M. Manjuladevi, R.K. Veena, V.S. Veena, Y.S. Koshkid'ko, and S. Sagar. Mater. Res. Bull. **145**, 111512 (2022). https://doi.org/10.1016/j.materresbull.2021.111512
[9] L.S. Sharath Chandra, A. Lakhani, D. Jain, S. Pandya, P.N. Vishwakarma, M. Gangrade, and V. Ganesan. Rev. Sci. Instrum. **79**, *10*, 103907 (2008). https://doi.org/10.1063/1.3002426
[10] Y. Sun, X. Xu, and Y. Zhang. J. Phys.: Condens. Matter **12**, *50*, 10475 (2000). https://doi.org/10.1088/0953-8984/12/50/309
[11] S. Banik, K. Das, T. Paramanik, N. Prasad Lalla, B. Satpati, K. Pradhan, and I. Das. NPG Asia Mater. **10**, 923 (2018). https://doi.org/10.1038/s41427-018-0085-7
[12] A. Mansingh and A. Dhawan. J. Phys. C **11**, *16*, 3439 (1978). http://dx.doi.org/10.1088/0022-3719/11/16/013
[13] Y. Kalyana Lakshmi, K. Raju, and P. Venugopal Reddy. J. Appl. Phys. **113**, *16*, 163701 (2013). https://doi.org/10.1063/1.4802436